Am J Transl Res 2023;15(10):6226-6233
www.ajtr.org /ISSN:1943-8141/AJTR0150783

Original Article

Artificial intelligence technology enhances the performance of shear wave elastography in thyroid nodule diagnosis

Jingmei Tuo[1], Xiaojuan Si[1], Heqin Song[2]

[1]*Department of Ultrasound Medicine, Zhangjiakou First Hospital, Zhangjiakou 330098, Hebei, China;*
[2]*Department of Laboratory Medicine, Zhangjiakou First Hospital, Zhangjiakou 330098, Hebei, China*

Received April 18, 2023; Accepted September 7, 2023; Epub October 15, 2023; Published October 30, 2023

Abstract: Objective: To investigate the diagnostic value of Artificial Intelligence (AI) in thyroid nodules diseases. Methods: This study included 100 patients (100 nodules - 23 benign; 77 malignant) who underwent shear wave elastography (SWE) and AI imaging of nodules prior to biopsy and/or surgery in Zhangjiakou First Hospital from January 2021 to December 2021. The image diagnostic value of AI was analyzed. Results: Among the 100 patients, there were 77 malignant nodules (77%) and 23 benign nodules (23%). Papillary thyroid carcinoma accounted for 94.8% (74/77) of the malignant nodules, and nodular goiter accounted for 100% of the benign nodules. The overall detection rate of AI+SWE was higher than that of SWE alone ($P < 0.05$). The accuracy, sensitivity, specificity, negative predictive value, and positive predictive value of AI+SWE were all higher than those of SWE only ($P < 0.05$). The ROC curve results showed that the area under the curve of AI+SWE in the diagnosis of thyroid nodules was 0.903. This was higher than that of SWE ($P < 0.05$). Conclusion: SWE+AI is effective in the diagnosis of thyroid nodules, and its sensitivity and specificity are better than those of SWE only.

Keywords: Artificial intelligence, shear wave elastography, thyroid nodules

Introduction

Thyroid nodular diseases include nodular goiter, thyroid adenoma, and thyroid cancer. Thyroid cancer is the most common malignant tumor of the head and neck [1]. According to Globocan 2012, there were 298,000 cases of thyroid cancer and 40,000 deaths from thyroid cancer worldwide in 2012, with a linear annual increase in recent decades [2-4]. In the face of the rapid increase in the incidence and mortality of thyroid cancer, early detection and timely treatment of the cancer before it expands and metastasizes is the key to improving the efficacy [5]. The development of imaging techniques to improve the recognition of thyroid nodular disease is an important task for medical professionals.

Ultrasonography is the method of choice for imaging thyroid nodular disease. Routine ultrasonography has a relatively high detection rate of thyroid nodules, up to 70% [6]. The detection ratio of palpation to ultrasound has been reported to be 1:5 for thyroid nodules, and 1:2 when the diameter of the nodule exceeds 2 cm [7]. For thyroid nodules greater than 1 cm in diameter, a previous study reported that 46% of nodules were not detected on surgical physical examination but were detected by ultrasound [8]. Benign thyroid nodules are involved in a variety of diseases, such as nodular goiter, adenoma, and thyroiditis. Thyroid cancer includes different pathologic subtypes, and nodules of the same pathologic type and have different ultrasonographic manifestations at different disease stages [9]. As a result, the ultrasound presentations of benign and malignant thyroid nodules are varied and intersecting, leading to shortcomings in the diagnosis of thyroid nodules using a single modality [10]. Conventional ultrasound has a high detection rate of thyroid nodules but lacks specificity and sensitivity in differentiating between benign and malignant thyroid nodules. Different ultrasound modalities reflect different aspects of

the nature of thyroid nodules. Their combined application can complement each other and provide more information for the diagnosis of thyroid nodules. The value of ultrasound and real-time shear wave elastography (SWE) in thyroid-related studies has been increasingly recognized. The combination of ultrasound technology with multiple diagnostic modalities is expected to increase the detection rate of malignant nodules and decrease the misdiagnosis rate of benign nodules [11-13]. This could be a promising area of research in the coming years. Ultrasonography is an important adjunct to sensitively detect the microvasculature within thyroid nodules and to characterize the microcirculation within the nodule [14]. Studies have shown that rapid entry, rapid peak attainment, polyphasic washout curves, inhomogeneous enhancement, and long washout times are characteristic of malignant nodules as observed by imaging techniques [15-17]. SWE is a new ultrasound technique used to objectively assess tissue stiffness, reflecting information on the biomechanical aspects of thyroid nodules. It can be used in conjunction with conventional ultrasound techniques to improve diagnostic accuracy [18-20]. Higher elasticity scores and higher strain ratios indicate a greater likelihood of malignancy in thyroid nodules. More studies are reporting the use of multimodal ultrasound for the diagnosis of thyroid nodules. A previous study investigated the value of multimodal ultrasound in the diagnosis of micropapillary thyroid carcinoma in the elderly. It found that the sensitivity of ultrasound diagnosis was 80.68%, specificity was 62.20%, and accuracy was 71.76%. The sensitivity of multimodal ultrasound diagnosis was 92.63%, specificity was 81.33%, and accuracy was 87.65% [21]. The concordance between multimodal ultrasound diagnosis and pathologic diagnosis was high. The difference between multimodal ultrasound diagnosis and ultrasound alone was significant. Pei et al [22] explored the diagnostic value of conventional ultrasound combined with multimodal ultrasound for moderately and highly suspicious malignant nodules in the thyroid gland. Their findings showed that the combination of ultrasonography and SWE techniques significantly improved the sensitivity, specificity, accuracy, positive predictive value, and negative predictive value of conventional ultrasound. This suggested that the combined approach had clear value and deserved to be recognized in clinical practice.

Artificial Intelligence (AI) is a general description of human-like intelligent activities such as computer simulation of human thinking and behavior. This included methods or techniques such as machine learning, artificial neural networks, and deep learning. Artificial intelligence has been applied to medical imaging to perform functions such as detection, classification, quantification, or prioritization [23]. Artificial intelligence-assisted diagnosis is an important branch of artificial intelligence technology in medical applications. This helped to improve the detection rate and diagnostic performance of lesions. The application of artificial intelligence-assisted diagnosis mainly includes two major functions: detection and classification. Detection: The detection rate of ultrasound examination is greatly affected by the operator's technology. When the operator is inexperienced, it is easier to cause missed diagnosis. Artificial intelligence-assisted diagnosis can improve the detection rate of lesion areas and reduce the false-negative rate by locating abnormal or suspicious areas in the image [24, 25]. Classification: As benign and malignant tumor features have commonality, difference, and intersectionality, identification on ultrasound only by the naked eye and experience can easily cause misdiagnosis. Based on the correlation between thyroid cancer image features and the type of pathology, the use of AI-assisted diagnosis of thyroid cancer images can help classify the diagnosis by quantifying the tumor features and obtaining a qualitative interpretation [26]. Studies have been conducted to combine AI techniques with conventional ultrasound techniques. Li et al [27] performed imaging histology based on the heterogeneity of liver echotexture on conventional ultrasound images to quantify the extent of liver fibrosis based on its area. Using this method, they were able to accurately differentiate between the F0-3 and F4-6 stages of hepatic fibrosis with an area under the ROC curve (AUC) of 98.5%, specificity of 93.3%, and sensitivity of 93.7%. The aim of this study was to investigate the diagnostic value of AI in thyroid nodules diseases, to provide additional assistance to healthcare professionals in diagnosing thyroid nodules.

Methods and materials

Study design and ethics

Data of 100 patients with thyroid nodular disease treated in Zhangjiakou First Hospital from January 2021 to December 2021 were retrospectively collected. This study has been reviewed and approved by the medical ethics committee of Zhangjiakou First Hospital.

All the patients received AI conventional ultrasonography and SWE examinations. The diagnostic values of SWE only and AI+SWE were compared. The results of pathological examinations were used as the gold standard for the diagnostic efficacy of each method.

Inclusion

(1) Patients who were 18 years old or older; (2) Patients with thyroid nodules ≥ 1 cm in diameter; (3) Patients with thyroid nodules scheduled for surgical removal, and their nodules had definite pathological findings; (4) Patients with complete clinical information; (5) Patients with thyroid nodular disease who underwent SWE and AI imaging of nodules prior to biopsy and/or surgery.

Exclusion criteria

(1) Patients with a history of mental illness; (2) Patients with a family history of thyroid cancer, or a radiation exposure in childhood or adolescence; (3) Patients with a previous history of thyroid surgery; (4) Patients with incomplete clinical data; (5) Patients with mixed echogenic lesions (cystic component > 80%), or anechoic lesions; (6) Pregnant or lactating women; (7) Patients with impaired consciousness and unable to communicate effectively.

Techniques

After completion of the examinations, all patients underwent surgery or puncture for biopsy, and pathological results were obtained after biopsy of the specimens.

AI conventional ultrasonography: The examination was performed using the version 2.0 AI-SONICTM thyroid nodule artificial intelligence assisted diagnosis system (DEMETICS ultrasound diagnostic robot, Zhejiang Deshan Yunxing Medical Technology Co.). Procedure Routine ultrasound examination of the thyroid gland was performed by two sonographers with many years of experience in thyroid ultrasound diagnosis, using a HITACHI-AR70 color Doppler ultrasound diagnostic instrument manufactured by Hitachi, Japan, with a probe model L12-2 and a frequency of 5-13 Hz. The system parameters were kept unchanged. The gain was 30 dB and the time gain compensation was intermediate (zero compensation). The operation was supervised and guided by two surgeons (Jingmei Du and Xiaojuan Si) and an application engineer from AI Automated Inspection Systems, Inc. to obtain the best standardized ultrasound sectional view images. The surgeons transmitted the scanned images to the server by a capture card or DICOM. Artificial intelligence algorithms automatically quantify five characteristics of thyroid nodules: size, borders, morphology, internal echogenicity, and foci of calcification. Each nodule is displayed in 4 separate longitudinal and transverse views and is static save and transmitted to the automated interpretation system in real time until the Thyroid Imaging Reporting and Data System (TI-RADS) values stabilize and the system automatically interprets the nodule's highest risk probability value.

SWE: All patients underwent routine ultrasonography to observe the location, size, morphology, borders, internal echogenicity, calcification, attenuation, and peripheral and internal blood supply of each nodule. The optimal section was selected and the probe was fixed without pressure. The patient was asked to hold his/her breath while the SWE imaging mode was activated. The Young's modulus value was measured and preset to 0-100 kPa. The SWE imaging area is set to cover as much of the nodule and surrounding normal thyroid tissue as possible. After the imaging area had stabilized for 3 seconds, the image was frozen and the Q-BOXTM function was activated to determine the maximum (Emax) and mean (Emean) values of the elastic modulus of the thyroid nodule in the sampling frame. The procedure was repeated 3 times by an experienced sonographer and the average value was taken.

Diagnostic criteria

AI Conventional ultrasound has a risk probability value of 0-1, where 0 to 0.39 is on the benign

Table 1. The baseline data of all subjects

	Subjects (n=100)
Age (years)	45.7±5.32
Sex	
Male (n%)	18 (18%)
Female (n%)	82 (82%)
BMI	17.95±1.43
Benign	23 (23%)
Nodular goiter	23 (23%)
Thyroid adenomatoid nodules	0
Subacute thyroiditis	0
Hashimoto's thyroiditis	0
Malignant	77 (77%)
Papillary thyroid carcinoma	74 (74%)
Medullary thyroid carcinoma	1 (1%)
Thyroid follicular carcinoma	1 (1%)
Undifferentiated thyroid carcinoma	0
Goiter nodularis	1 (1%)
TIRADS classification	
I	19 (19%)
II	20 (20%)
III	23 (23%)
IVa	21 (21%)
IVb	14 (14%)
IVc	3 (3%)

Note: BMI: body mass index.

Table 2. Comparison of diagnostic results of different examinations for thyroid nodules

Diagnostic examinations	Benign thyroid nodules (n=23)	Malignant thyroid nodules (n=77)
AI+SWE	19 (82.6%)	73 (94.8%)
SWE	12 (52.2%)	59 (76.6%)
χ^2/t	5.456	7.653
P	0.021	0.011

Note: AI: Artificial Intelligence; SWE: shear wave elastography.

side (no malignant features), 0.40 to 0.59 is suspected malignancy (presence of a tendency to malignant features), and 0.60 to 1 is on the malignant side (presence of malignant features). A value of 0.40 was considered the threshold for the diagnosis of malignancy.

For SWE, the quantitative diagnostic criteria for benign and malignant thyroid nodules were based on the Guidelines for the Clinical Application of Ultrasound Electron Imaging. Thyroid nodules with a reference threshold Emax ≥ 46.1 kPa Esd ≥ 5.8 were considered malignant [28].

Statistical analysis

Statistical data were analyzed using SPSS 23.0. Counted data were expressed as cases (percentages) [n (%)] and analyzed by χ^2 test. Measured data were expressed as mean ± standard deviation (Mean ± sd) and analyzed by independent samples t-test. Kappa analysis was used for consistency analysis. Receiver operator characteristic curves (ROC) were plotted. The AUCs were compared using Z test. All test levels were set as two-sided α=0.05, and $P < 0.05$ was the criterion for evaluating the differences as significant.

Results

Clinical characteristics

Among the 100 patients, there were 77 malignant nodules (77%) and 23 benign nodules (23%) (**Table 1**). Papillary thyroid carcinoma accounted for 94.8% (74/77) of the malignant nodules. Nodular goiter accounted for 100% of the benign nodules.

Comparison of diagnostic results of different examinations for thyroid nodules

In the diagnosis of thyroid nodules, the overall detection rate of AI+SWE was higher than that of SWE ($P < 0.05$) (**Table 2**).

Analysis of different detection results

The accuracy, sensitivity, specificity, negative predictive value, and positive predictive value of AI+SWE were higher than those of SWE ($P < 0.05$) (**Table 3**).

ROC curve analysis

The ROC curve showed that the AUC of AI+SWE in diagnosing thyroid nodules was 0.903. This was higher than that of SWE ($P < 0.05$) (**Figure 1**).

The representative ultrasound images of two groups

Figure 2 presents some typical thyroid images of two groups. The SWE image of benign thyroid nodule showed that the shape of the nodules was regular, with a complete capsule. The inte-

Table 3. Analysis of different detection results

Group	SWE (n=100)	AI+SWE (n=100)	t	*P*
Accuracy	60.78%	90.3%	13.123	0.004
Sensitivity	60.1%	89.9%	7.128	0.002
Specificity	65%	94%	5.217	0.015
Negative predictive value	86%	97%	7.347	0.007
Positive predictive value	35%	76%	13.009	0.002

Note: AI: Artificial Intelligence; SWE: shear wave elastography.

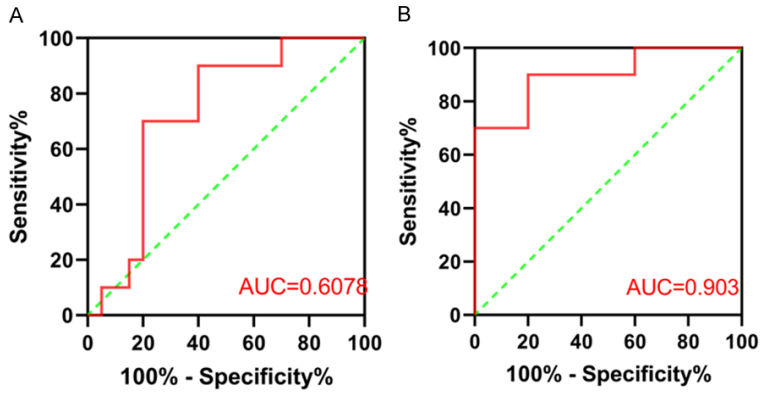

Figure 1. The ROC analysis. A: The ROC curve of SWE; B: The ROC curve of AI+SWE. Note: AI: Artificial Intelligence; SWE: shear wave elastography.

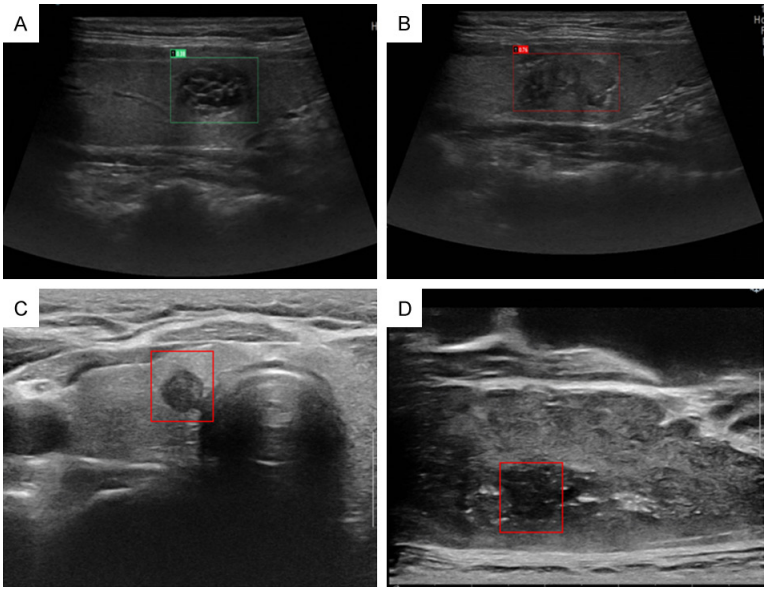

Figure 2. The representative ultrasound images of two groups. A, B. The images of AI+SWE group; C, D. The images of SWE group. Note: AI: Artificial Intelligence; SWE: shear wave elastography.

rior of the nodules presented isoechogenicity, and complete sound halos were seen around the nodules (**Figure 2C**). The SWE image of malignant thyroid nodules showed that the shape of the nodule was irregular, with no obvious or incomplete capsule. The interior of the nodule was often hypoechoic (**Figure 2D**). The SWE+AI image of the benign thyroid nodule indicated that the nodule had a regular morphology and a complete capsule. The interior of the nodule can exhibit high echo, mixed echo, and low echo. The aspect ratio of the nodule was less than 1, and complete sound halos were seen around the nodule (**Figure 2A**). The SWE+AI image of malignant thyroid nodule showed that the nodule was irregular, with no obvious or incomplete capsule. The interior of the nodule was often hypoechoic, and some of the echoes behind the nodule attenuated. The ratio of the longitudinal and transverse diameters of the nodule was greater than or equal to 1, and small calcifications were seen inside the nodule (**Figure 2B**).

Discussion

Many studies have investigated the diagnostic efficacy of AI-assisted diagnostic systems. Wang et al [29] utilized 21,532 images from 5,842 patients to automatically detect thyroid nodules using a cascaded convolutional neural network. They designed a model that bypasses errors that can occur during preprocessing. This can lead to inaccurate results and classification bias due to lack of robustness of the feature set. Their model has good detection efficiency with an AUC of 98.51%. Liang et al [30] used a multiscale detection network to auto-

matically detect thyroid nodules with an accuracy of 97.5%. Xie et al [31] concluded that the AmCAD-UT detection system in the AI-assisted diagnostic system hads high sensitivity for the diagnosis of nodules in Hashimoto's thyroiditis. It had a low specificity, and was prone to overdiagnosis. Sorrenti [32] reported that artificial intelligence-assisted diagnostic systems have relatively low sensitivity but high specificity in the differential diagnosis of thyroid nodules. This is worthy of clinical dissemination. Xiang et al [33] proposed a computer-assisted diagnostic system called ThyroScan. This utilized thyroid gland from 232 normal thyroid and 294 Hashimoto's thyroiditis patients' images with seven important wavelet features extracted from the images. The fuzzy classifier detected Hashimoto's thyroiditis with an accuracy of up to 85%, making it significant and accurate in the clinical diagnosis of thyroid diseases. In this study, AI was combined with SWE for the first time to diagnose benign and malignant thyroid nodules. The results showed that SWE combined with AI was more sensitive and accurate than SWE alone. It was expected to be one of the noninvasive tests for diagnosing thyroid nodules.

There are several key points in the diagnosis of AI+SWE. 1) Number of masses or nodules: benign thyroid masses, such as nodular goiters, tend to be bilateral, multiple, and diffusely distributed. Thyroid carcinomas tend to be unilateral and solitary. 2) Envelope and borders of the mass: benign thyroid masses, such as nodular masses, have non-smooth borders and no envelope. Thyroid adenoma masses have smooth borders and an envelope. 3) Internal echo of the mass: the internal echo of nodular goiter is mainly mixed echo, the internal echo of thyroid adenoma is more homogeneous. The internal echo of thyroid adenocarcinoma is mainly hypoechoic and inhomogeneous. 4) Blood flow: the blood supply of nodular goiter tissues is mainly grade I, with a regular vascular course. The adenoma can be seen as a ring with richer blood flow signals. Malignant tumors have a disturbed distribution of blood vessels in and around the tumor. Blood flow is abundant. 5) Whether calcification: calcification is more common in malignant tumors.

This study had several limitations. This had a retrospective design, and selection bias may have been unavoidable in this study. The study population was small. The cost-effectiveness of AI+SWE and SWE were not evaluated in this study. Larger randomized controlled clinical trials are needed to obtain more evidence.

SWE+AI is effective in the diagnosis of thyroid nodules, and its sensitivity and specificity are higher than that of SWE.

Acknowledgements

This work was supported by 2022 Medical Science Research Project Plan of Hebei Province (No. 20221902).

Disclosure of conflict of interest

None.

Address correspondence to: Jingmei Tuo, Department of Ultrasound Medicine, Zhangjiakou First Hospital, No. 6 Mosque Lane, Xinhua Front Street, Qiaoxi District, Zhangjiakou 330098, Hebei, China. Tel: +86-15930340662; E-mail: tuojingmei112@163.com

References

[1] Unnikrishnan AG. Nodular diseases in the thyroid. J Assoc Physicians India 2011; 59 Suppl: 43-45.

[2] Ferlay J, Soerjomataram I, Dikshit R, Eser S, Mathers C, Rebelo M, Parkin DM, Forman D and Bray F. Cancer incidence and mortality worldwide: sources, methods and major patterns in GLOBOCAN 2012. Int J Cancer 2015; 136: E359-386.

[3] Torre LA, Bray F, Siegel RL, Ferlay J, Lortet-Tieulent J and Jemal A. Global cancer statistics, 2012. CA Cancer J Clin 2015; 65: 87-108.

[4] Salamanca-Fernández E, Rodriguez-Barranco M, Chang-Chan YL, Redondo-Sanchez D, Dominguez-Lopez S, Bayo E, Narankiewicz D, Expósito J and Sánchez MJ. Thyroid Cancer Epidemiology in South Spain: a population-based time trend study. Endocrine 2018; 62: 423-431.

[5] Brose MS, Bible KC, Chow LQM, Gilbert J, Grande C, Worden F and Haddad R. Management of treatment-related toxicities in advanced medullary thyroid cancer. Cancer Treat Rev 2018; 66: 64-73.

[6] Li F and Luo H. Comparative study of thyroid puncture biopsy guided by contrast-enhanced ultrasonography and conventional ultrasound. Exp Ther Med 2013; 5: 1381-1384.

[7] Tarigan TJE, Anwar BS, Sinto R and Wisnu W. Diagnostic accuracy of palpation versus ultrasound-guided fine needle aspiration biopsy for

diagnosis of malignancy in thyroid nodules: a systematic review and meta-analysis. BMC Endocr Disord 2022; 22: 181.
[8] Huang X, Qiu Y, Chen Y, Chen L, Yi J and Luo X. Epidemiological survey of thyroid nodules in 2098 patients for routine physical examination in Fujian, China. Contrast Media Mol Imaging 2022; 2022: 2913405.
[9] Durante C, Costante G, Lucisano G, Bruno R, Meringolo D, Paciaroni A, Puxeddu E, Torlontano M, Tumino S, Attard M, Lamartina L, Nicolucci A and Filetti S. The natural history of benign thyroid nodules. JAMA 2015; 313: 926-935.
[10] Zhao SX, Chen Y, Yang KF, Luo Y, Ma BY and Li YJ. A local and global feature disentangled network: toward classification of benign-malignant thyroid nodules from ultrasound image. IEEE Trans Med Imaging 2022; 41: 1497-1509.
[11] Koundal D, Gupta S and Singh S. Computer-aided diagnosis of thyroid nodule: a review. International Journal of Computer Science and Engineering Survey 2012; 3: 67.
[12] Lv K, Cao X, Dong Y, Geng D and Zhang J. CT/MRI LI-RADS version 2018 versus CEUS LI-RADS version 2017 in the diagnosis of primary hepatic nodules in patients with high-risk hepatocellular carcinoma. Ann Transl Med 2021; 9: 1076.
[13] Zhao L, Pang P, Zang L, Luo Y, Wang F, Yang G, Du J, Wang X, Lyu Z, Dou J and Mu Y. Features and trends of thyroid cancer in patients with thyroidectomies in Beijing, China between 1994 and 2015: a retrospective study. BMJ Open 2019; 9: e023334.
[14] Zhan J and Ding H. Application of contrast-enhanced ultrasound for evaluation of thyroid nodules. Ultrasonography 2018; 37: 288-297.
[15] Survarachakan S, Prasad PJR, Naseem R, Pérez de Frutos J, Kumar RP, Langø T, Alaya Cheikh F, Elle OJ and Lindseth F. Deep learning for image-based liver analysis - A comprehensive review focusing on malignant lesions. Artif Intell Med 2022; 130: 102331.
[16] Speidel A, Bisterov I, Saxena KK, Zubayr M, Reynaerts D, Natsu W and Clare AT. Electrochemical jet manufacturing technology: from fundamentals to application. Int J Mach Tools Manuf 2022; 2022: 103931.
[17] Kaya A and Can AB. A weighted rule based method for predicting malignancy of pulmonary nodules by nodule characteristics. J Biomed Inform 2015; 56: 69-79.
[18] Piscaglia F, Salvatore V, Mulazzani L, Cantisani V and Schiavone C. Ultrasound shear wave elastography for liver disease. A critical appraisal of the many actors on the stage. Ultraschall Med 2016; 37: 1-5.
[19] Nadebaum DP, Nicoll AJ, Sood S, Gorelik A and Gibson RN. Variability of liver shear wave measurements using a new ultrasound elastographic technique. J Ultrasound Med 2018; 37: 647-656.
[20] Popa A, Șirli R, Popescu A, Bâldea V, Lupușoru R, Bende F, Cotrău R and Sporea I. Ultrasound-based quantification of fibrosis and steatosis with a new software considering transient elastography as reference in patients with chronic liver diseases. Ultrasound Med Biol 2021; 47: 1692-1703.
[21] Addley S, Mihai R, Alazzam M, Dhar S and Soleymani Majd H. Malignant struma ovarii: surgical, histopathological and survival outcomes for thyroid-type carcinoma of struma ovarii with recommendations for standardising multi-modal management. A retrospective case series sharing the experience of a single institution over 10 years. Arch Gynecol Obstet 2021; 303: 863-870.
[22] Pei S, Cong S, Zhang B, Liang C, Zhang L, Liu J, Guo Y and Zhang S. Diagnostic value of multimodal ultrasound imaging in differentiating benign and malignant TI-RADS category 4 nodules. Int J Clin Oncol 2019; 24: 632-639.
[23] Lewis SJ, Gandomkar Z and Brennan PC. Artificial intelligence in medical imaging practice: looking to the future. J Med Radiat Sci 2019; 66: 292-295.
[24] Sechopoulos I, Teuwen J and Mann R. Artificial intelligence for breast cancer detection in mammography and digital breast tomosynthesis: state of the art. Semin Cancer Biol 2021; 72: 214-225.
[25] Yoo H, Lee SH, Arru CD, Doda Khera R, Singh R, Siebert S, Kim D, Lee Y, Park JH, Eom HJ, Digumarthy SR and Kalra MK. AI-based improvement in lung cancer detection on chest radiographs: results of a multi-reader study in NLST dataset. Eur Radiol 2021; 31: 9664-9674.
[26] Wei X, Zhu J, Zhang H, Gao H, Yu R, Liu Z, Zheng X, Gao M and Zhang S. Visual interpretability in computer-assisted diagnosis of thyroid nodules using ultrasound images. Med Sci Monit 2020; 26: e927007.
[27] Li J, Qureshi M, Gupta A, Anderson SW, Soto J and Li B. Quantification of degree of liver fibrosis using fibrosis area fraction based on statistical chi-square analysis of heterogeneity of liver tissue texture on routine ultrasound images. Acad Radiol 2019; 26: 1001-1007.
[28] Pei S, Zhang B, Cong S, Liu J, Wu S, Dong Y, Zhang L and Zhang S. Ultrasound real-time tissue elastography improves the diagnostic performance of the ACR thyroid imaging reporting and data system in differentiating malignant from benign thyroid nodules: a summary of

1525 thyroid nodules. Int J Endocrinol 2020; 2020: 1749351.
[29] Wang D, Wang HX, Lu F, Li XL, Guo LH, Zhao CK, Sun LP, Fu HJ, Zhang YF and Xu HX. Ultrasound-based computer-aided diagnosis for cytologically indeterminate thyroid nodules with different radiologists. Clin Hemorheol Microcirc 2022; 82: 217-230.
[30] Liang X, Huang Y, Cai Y, Liao J and Chen Z. A computer-aided diagnosis system and thyroid imaging reporting and data system for dual validation of ultrasound-guided fine-needle aspiration of indeterminate thyroid nodules. Front Oncol 2021; 11: 611436.
[31] Xie F, Luo YK, Lan Y, Tian XQ, Zhu YQ, Jin Z, Zhang Y, Zhang MB, Song Q and Zhang Y. Differential diagnosis and feature visualization for thyroid nodules using computer-aided ultrasonic diagnosis system: initial clinical assessment. BMC Med Imaging 2022; 22: 153.
[32] Sorrenti S, Dolcetti V, Radzina M, Bellini MI, Frezza F, Munir K, Grani G, Durante C, D'Andrea V, David E, Calò PG, Lori E and Cantisani V. Artificial intelligence for thyroid nodule characterization: where are we standing? Cancers (Basel) 2022; 14: 3357.
[33] Xiang Z, Zhuo Q, Zhao C, Deng X, Zhu T, Wang T, Jiang W and Lei B. Self-supervised multimodal fusion network for multi-modal thyroid ultrasound image diagnosis. Comput Biol Med 2022; 150: 106164.